

Effect of trace oxygen on plasma nitriding of titanium foil

Hai-Tao Zhou(周海涛), Xi-Ya Xiong(熊希雅), Ke-Xin Ma(马可欣), Bing-Wei Luo(罗炳威), Fei Luo(罗飞), Cheng-Min Shen(申承民)

Citation: Chin. Phys. B, 2024, 33 (**6**): 068103. DOI: 10.1088/1674-1056/ad35b0
Journal homepage: http://cpb.iphy.ac.cn; http://iopscience.iop.org/cpb

What follows is a list of articles you may be interested in

Characterization of the N-polar GaN film grown on C-plane sapphire and misoriented C-plane sapphire substrates by MOCVD

Xiaotao Hu(胡小涛), Yimeng Song(宋祎萌), Zhaole Su(苏兆乐), Haiqiang Jia(贾海强), Wenxin Wang(王文新), Yang Jiang(江洋), Yangfeng Li(李阳锋), and Hong Chen(陈弘)
Chin. Phys. B, 2022, 31 (**3**): 038103. DOI: 10.1088/1674-1056/ac3bad

Effect of hydrogen content on dielectric strength of the silicon nitride film deposited by ICP-CVD

Yudong Zhang(张玉栋), Jiale Tang(唐家乐), Yongjie Hu(胡永杰), Jie Yuan(袁杰), Lulu Guan(管路路), Xingyu Li(李星雨), Hushan Cui(崔虎山), Guanghui Ding(丁光辉), Xinying Shi(石新颖), Kaidong Xu(许开东), and Shiwei Zhuang(庄仕伟)
Chin. Phys. B, 2021, 30 (**4**): 048103. DOI: 10.1088/1674-1056/abea82

Multi-layer structures including zigzag sculptured thin films for corrosion protection of AISI 304 stainless steel

Fateme Abdi
Chin. Phys. B, 2021, 30 (**3**): 038106. DOI: 10.1088/1674-1056/abd398

Density functional calculations of efficient H_2 separation from impurity gases (H_2, N_2, H_2O, CO, Cl_2, and CH_4) via bilayer g-C_3N_4 membrane

Yuan Guo(郭源), Chunmei Tang(唐春梅), Xinbo Wang(王鑫波), Cheng Wang(王成), Ling Fu(付玲)
Chin. Phys. B, 2019, 28 (**4**): 048102. DOI: 10.1088/1674-1056/28/4/048102

Superlubricity enabled dry transfer of non-encapsulated graphene

Zhe Ying(应哲), Aolin Deng(邓奥林), Bosai Lyu(吕博赛), Lele Wang(王乐乐), Takashi Taniguchi, Kenji Watanabe, Zhiwen Shi(史志文)
Chin. Phys. B, 2019, 28 (**2**): 028102. DOI: 10.1088/1674-1056/28/2/028102

Effect of trace oxygen on plasma nitriding of titanium foil

Hai-Tao Zhou(周海涛)[1], Xi-Ya Xiong(熊希雅)[1], Ke-Xin Ma(马可欣)[1], Bing-Wei Luo(罗炳威)[1], Fei Luo(罗飞)[1], and Cheng-Min Shen(申承民)[2,†]

[1] *Beijing Institute of Aeronautical Materials, Aero Engine Corporation of China, Beijing* 100095, *China*
[2] *Beijing National Laboratory of Condensed Matter Physics, Institute of Physics, Chinese Academy of Sciences, Beijing* 100190, *China*

(Received 18 January 2024; revised manuscript received 5 March 2024; accepted manuscript online 20 March 2024)

Titanium nitride films are prepared by plasma enhanced chemical vapor deposition method on titanium foil using N_2 as precursor. In order to evaluate the effect of oxygen on the growth of titanium nitride films, a small amount of O_2 is introduced into the preparation process. The study indicates that trace O_2 addition into the reaction chamber gives rise to significant changes on the color and micro-morphology of the foil, featuring dense and long nano-wires. The as-synthesized nanostructures are characterized by various methods and identified as TiN, Ti_2N, and TiO_2 respectively. Moreover, the experiment results show that oxide nanowire has a high degree of crystallinity and the nitrides present specific orientation relationships with the titanium matrix.

Keywords: nitride, oxide, nanostructure, crystalline, plasma-enhanced chemical vapor deposition system (PECVD)

PACS: 81.15.Gh, 61.46.Km, 61.46.Df **DOI:** 10.1088/1674-1056/ad35b0

1. Introduction

Plasma nitriding technology has been widely used in industrial and medical areas to improve the poor tribological properties of titanium alloy.[1–8] One study by Tarnowski *et al.* discussed that the nitride layer presented many advantages such as low coefficient of friction, low penetration depth and good adhesion to the matrix.[1] The investigation by Yilbas *et al.* showed that TiN/Ti_2N layers were formed after nitriding treatment and the wear resistance was considerably increased via pin-on-disc wear test.[2] In Tamura's work, the outstanding mechanical properties of nitrided titanium were evaluated by various tests and verified via hypodermic implantation.[3] Lakshmi *et al.* reported that titanium alloy was nitrided by direct-current plasma method and the coating showed higher anti-corrosion property in acid environment.[6] Therefore, the nitriding process could significantly improve the anti-wear and anti-corrosion properties of the titanium alloys.

In the nitriding process, the leakage of air and O_2 into the reaction system is inevitable, and the reaction tends to form titanium oxide rather than nitride due to the more active feature of O_2.[9] The hardness of oxidized surface is much lower than that of nitrided, with the values of around 1000 HV and up to 3000 HV respectively, which will give rise to the degradation of the surface wear resistance.[10–12] Consequently, it is worth to study the effect of oxygen on the nitriding process from the microscopic perspective, however few works focus on this issue. In this brief report, we studied the influence of oxygen on the microstructure, morphology and composition of TiN films, through adding trace O_2 into N_2 in the plasma-assisted chemical reaction. By employing various analysis methods, the crystalline phase and micro-morphology of the coating layer were investigated in details. These results have further significance for the preparation of high quality TiN films by plasma nitriding.

2. Experimental procedure

2.1. Preparation of titanium nitride on titanium foil

The experiment was carried out in a home-built plasma-enhanced chemical vapor deposition system (PECVD), the pressure of which was pumped to 1×10^{-1} Pa, as shown in Fig. 1. The leakage of the oxygen is estimated at 0.00134 sccm via comparing the vacuum variations due to the leakage and intentional introduction (see supporting information for details). The titanium (Ti) foil was placed in the middle of the furnace, and the nitrogen (N_2) or oxygen (O_2) gas was ionized by the plasma coil at the upstream. The vacuum inside the quartz tube was tuned by the flow controller and mechanical pump. Firstly, the titanium foil was heated to 750 °C at a rate of 20 °C/min under the protection of argon gas (Ar, 300 sccm, standard cubic centimeter per minute). Then the argon flow was shut down and N_2/O_2 was introduced into the tube with turning on the radio frequency (RF) source at a power of 300 W. After treatment for 60 min, the heating and RF source were turned off and the inside atmosphere was shift back to Ar.

†Corresponding author. E-mail: cmshen@iphy.ac.cn

© 2024 Chinese Physical Society and IOP Publishing Ltd

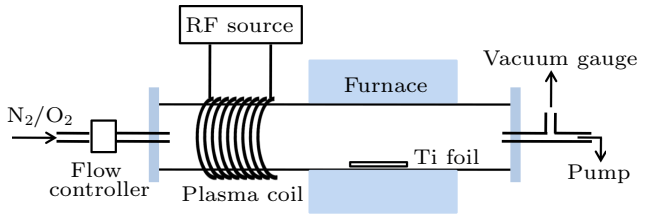


Fig. 1. The schematic illustration of the plasma-enhanced chemical vapor deposition system.

2.2. Characterizations

The microstructure of the sample was characterized by scanning electron microscope (SEM, Hitachi S-4800) and high resolution transmission electron microscope (HRTEM, FEI Tecai G2F20). The x-ray photoelectron spectroscopy (XPS) analysis was conducted on Thermoescalab 250XI, utilizing monochromatized Al-$K\alpha$ radiation at 150 W. The high resolution XPS spectra were recorded in the CAE mode with a pass energy of 20 eV and a step size of 0.1 eV. The x-ray diffraction (XRD) was carried out on Bruker D8, using Cu $K\alpha$ rays with a wavelength of 0.154 nm and a scanning rate of 6°/min.

3. Results and discussion

Figures 2(a) and 2(b) are the photo images of the titanium foil after being treated by N_2 (10 sccm) and N_2/O_2 (10/0.1 sccm), showing the colors of yellow and blue respectively. These images indicate that tiny amount of oxygen can give rise to significant change of the reactions at the surface of Ti foil. XPS is carried out to study the chemical compositions of the two samples, as presented in Fig. 2(c) and Table 1. From which we can obtain the atomic ratios of the nitride to oxide are about 2:1 and 1:20 in yellow and blue samples respectively. The blue surface consists of fewer nitrogen and twice percent of oxygen compared with the yellow surface, proving that O_2 is the key factor to the color difference.

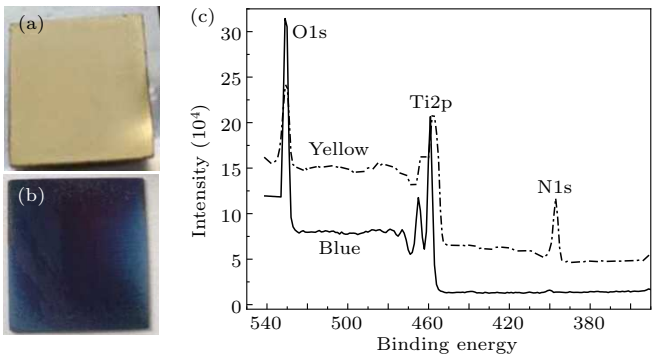


Fig. 2. (a)and (b) Photo images of the titanium foil after being treated by N_2 and N_2/O_2 respectively. (c) XPS curves of the yellow and blue surfaces.

The XPS analysis is surface-sensitive and only able to test the sample several nanometers underneath the surface. Therefore, we further carry out XRD measurement which has the capability to detect much deeper of several micrometers and get information about the crystal structure. The result is shown in Fig. 3 and peaks are identified as TiO_2, Ti_2N, and TiN, indicating that the oxidation and nitridation occur on both yellow and blue surfaces. The O_2 is not intentionally introduced in the preparation of the yellow sample, and the probable source is the minor leakage of the vacuum system which is estimated at 0.00134 sccm. It is obvious that the intensity of TiO_2 peak (labeled by square) on blue surface is higher than that on yellow surface, implying much more oxidation structures are formed in the mixing N_2/O_2 (10/0.1 sccm) condition. It should be pointed that the O_2 flow of 0.1 sccm is the highest accuracy of the flow-controller, therefore the minimum threshold value of O_2 flow for bringing in the color change to blue is difficult to provide.

Table 1. Chemical compositions of the yellow and blue surfaces by XPS measurement.

	Binding energy (eV)	Atomic percent (%) (yellow surface)	Atomic percent (%) (blue surface)
N1s	397.16	21.67	1.04
Ti2p	457.64	24.41	22.82
O1s	530	22.53	46.81

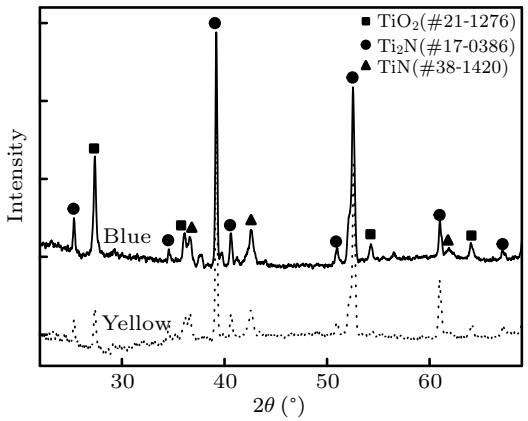


Fig. 3. XRD curves of the yellow and blue surfaces, indicating structures of TiO_2, Ti_2N, and TiN are formed on both surfaces.

The SEM measurement is used to characterize the micromorphology of the samples. As shown in Figs. 4(a) and 4(b), the yellow and blue surfaces feature sparse and dense nanowires, respectively. According to previous report, the titanium nitride usually shows the nanoparticle shape[13,14] while the titanium oxide tends to form nanowires.[15,16] Then it is reasonable to assign the nanowires as TiO_2 and the rough substrate as TiN or Ti_2N (labeled by arrows). In the experiment we find higher oxygen flow rate contributes to the faster growth of the nanowires, providing further evidence for above assignment (see Fig. S4 in supporting information). The length and width of the as-synthesized nanowires are around 1.5 μm and 50 nm. Moreover, the wires do not show obvious catalyst particles on their tips, indicating the growing process abides by the vapor–solid theory (VS) rather than vapor–liquid–solid (VLS).[16] During the reaction of titanium and

nitrogen, a large amount of heat is released and many titanium atoms or nano-particles are evaporated from the substrate surface at the elevated temperature. These evaporated titanium particles directly react with oxygen ions and form TiO_2 molecules, which subsequently self-assemble into nanowires on the substrate. The SEM results comply well with the aforementioned XRD analysis since the dense nanowires on blue surface give rise to higher peak weight of TiO_2. Post-oxidizing experiment is conducted by treating the grown yellow sample at 750 °C for 120 min with a 0.1-sccm flow of oxygen into the vacuum chamber. Although the O_2 is not ionized by RF, a blue sample is also obtained (shown in Fig. S1 in supporting information), further proving the high chemical sensitivity of titanium to oxygen.

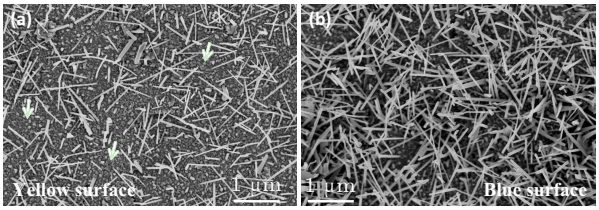


Fig. 4. (a) and (b) SEM images of the yellow and blue surfaces, featuring sparse and dense nanowires, respectively.

The effect of reaction time and temperature on the nitriding process is investigated. The SEM and XRD results indicate that the extension of time does not give rise to significant impact on the reaction products. The SEM image features the dense-nanowire morphology same as Fig. 4(b), and the XRD curves only present a minor decrease in the peak weight of Ti_2N when the nitriding time is extended to 120 min (labeled by arrows in Fig. S2 in supporting information). It is reasonable to interpret this decrease as follows, TiO_2 nanowires are grown above the Ti_2N layers, as the reaction time extending, more TiO_2 nanowires form and weaken the signal of Ti_2N at XRD detection. Contrast to time, temperature play an important role in the nitridation. As shown in Fig. S3 in supporting information, the TiN peak (labeled by arrow) does not appear in the XRD curves until the temperature is raised to 750 °C, indicating that the reaction barrier of TiN is much higher than that of Ti_2N and TiO_2.

We further utilize TEM to investigate the microstructures of TiO_2, Ti_2N, and TiN. The TiO_2 nanowire is picked out by tenderly scratching the blue surface with knife and ultrasonic dispersion in alcohol, while the Ti_2N/TiN sample is prepared by ion-beam thinning of the yellow surface. Figure 5(a) shows an image of single nanowire with a length of around 1.3 μm. This image further proves the lack of catalyst particle during the growth process. A high resolution image and corresponding diffraction pattern are presented in Figs. 5(b) and 5(c), from which the crystalline phase is determined as the rutile TiO_2 with tetragonal structure ($a = b = 0.4594$ nm, $c = 0.2959$ nm, $\alpha = \beta = \gamma = 90°$). This result also supports the assignment of nanowire as TiO_2 in the above SEM discussion. It is worth noting that this nanowire has a high degree of crystallinity and a twin structure with (01-1) as the twinning plane. Previously reported TiO_2 nanowire always exhibits a curled shape[16,17] and much effort has been devoted to grow straight wire.[18] Therefore, our work provides an alternative method to prepare straight titania nanowire without catalyst, which has potential applications as the anode in batteries or emitter in field emission.

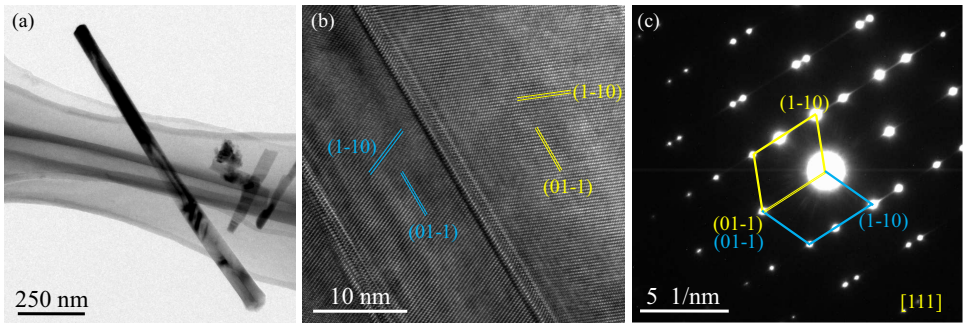


Fig. 5. The TEM image of single nanowire. (b) and (c) High resolution image and corresponding diffraction pattern of the TiO_2 nanowire in panel (a). [111] is the incident direction of the electron beam.

The yellow surface mainly consisting of titanium nitride is also investigated by TEM, and the diffraction spots are shown in Fig. 6. Two sets of patterns can be clearly identified in Fig. 6(a), which are labeled by solid and dashed parallelograms respectively. After carefully calculation, the solid pattern is assigned as α-phase Ti with hexagonal structure ($a = b = 0.2951$ nm, $c = 0.4683$ nm) and the other is Ti_2N with tetragonal structure ($a = b = 0.4945$ nm, $c = 0.3034$ nm). According to the above results, the crystal planes and incident directions are determined, from which we can further get the orientation relationship of Ti and Ti_2N, which are $(-112)_{Ti} \parallel (1\text{-}10)_{Ti2N}$ and $[201]_{Ti} \parallel [\text{-}1\text{-}1\text{-}1]_{Ti2N}$. Making the same analysis to Fig. 6(b), we can get two phases of α-phase Ti (solid) and cubic TiN ($a = b = c = 0.4242$ nm, dashed) with an orientation relation of $(110)_{Ti} \parallel (02\text{-}2)_{TiN}$ and $[\text{-}112]_{Ti} \parallel [011]_{TiN}$. From our discussion we have got a completely crystalline picture of

the titanium nitride, moreover, the information extracted from TEM results complies well with that provided by XRD, indicating the high accuracy of these measurements.

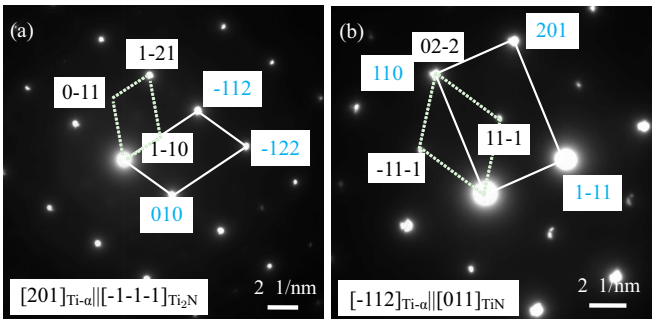


Fig. 6. (a) The TEM diffraction pattern with two phases of hexagonal Ti and tetragonal Ti_2N. (b) Diffraction pattern of hexagonal Ti and cubic TiN. The diffraction spots of Ti are labeled by solid parallelogram in both images.

4. Conclusion and perspectives

TiN, Ti_2N, and TiO_2 are grown on titanium foil using PECVD system. Titanium nitrides show yellow color, however, tiny addition of O_2 significantly changes the color to blue due to the formation of dense oxide nanowires. Combining XRD and TEM analysis methods, the crystalline phases of these nanostructures are determined. Furthermore, the as-prepared TiO_2 nanowire shows a high degree of crystallinity, and both of TiN and Ti_2N form specific crystal orientations with respect to Ti matrix. Our research presents numerous details about the effect of O_2 on the preparation of titanium nitride and may help to optimize the gas nitriding technology.

Acknowledgement

Project supported by the Innovation Funding of Beijing Institute of Aeronautical Materials.

References

[1] Tarnowski M, Borowski T, Skrzypek S, Kulikowski K and Wierzchoń T 2021 *J. Alloys Compd.* **864** 158896
[2] Yilbas B S, Sahin A Z, Al-Garni A Z, Said S A M, Ahmed Z, Abdulaleem B J and Sami M 1996 *Surf. Coat. Technol.* **80** 287
[3] Tamura Y, Yokoyama A, Watari F, Uo M and Kawasaki T 2002 *Mater. Trans.* **43** 3043
[4] Gil F J, Canedo R, Padros A and Sada E 2002 *J. Biomater. Appl.* **17** 31
[5] Czarnowska E, Wierzchon T and Maranda-Niedbala A 1999 *J. Mater. Process. Technol.* **92–93** 190
[6] Lakshmi S G, Arivuoli D and Ganguli B 2002 *Mater. Chem. Phys.* **76** 187
[7] Sagalovych A, Sagalovych V, Popov V, Dudnik S and Olijnyk O 2022 *Tribol. Mater.* **1** 106
[8] Zhang L, Shao M, Zhang Z, Yi X, Yan J, Zhou Z, Fang D, He Y and Li Y 2023 *Materials* **16** 2961
[9] Zhecheva A, Sha W, Malinov S and Long A 2005 *Surf. Coat. Technol.* **200** 2192
[10] Aniołek K, Kupka M and Barylski A 2016 *Wear* **356–357** 23
[11] Aniołek K 2017 *Vacuum* **144** 94
[12] Maytorena-Sánchez A, Hernández-Torres J, López-Huerta F, Hernández-Campos M A, Zamora-Peredo L, Pacio-Castillo M, Serrano-De L E and García-González L 2021 *Mater. Lett.* **282** 128679
[13] Ge W, Chang Z, Siddique A, Shi B and Liu C 2020 *Ceram. Int.* **46** 7355
[14] Kim H T, Kim M J and Sohn S H 2012 *J. Phys. Chem. Solids* **73** 931
[15] Daothong S, Songmee N, Thongtem S and Singjai P 2007 *Scripta Mater.* **57** 567
[16] Amin S S, Nicholls A W and Xu T T 2007 *Nanotechnology* **18** 445609
[17] Tao R, Wu J, Xue H, Song X, Pan X, Fang X, Fang X and Dai S 2010 *J. Power Sources* **195** 2989
[18] Du J, Gu X, Guo H, Liu J, Wu Q and Zou J 2015 *J. Cryst. Growth* **42** 754